Recoil Radiation Damage in Tungsten Compounds Observed Using the Mössbauer Effect Following Coulomb Excitation[*]

S. A. Wender[†] and N. Hershkowitz

Department of Physics and Astronomy, The University of Iowa, Iowa City, Iowa 52242

The short-time effects of irradiation upon WC, WB, W_2B, W_2B_5, WO_3, and WS_2 were studied by observing the Mössbauer effect of tungsten nuclei following Coulomb excitation with 6-MeV α particles. Values for the recoilless fraction, hyperfine interaction, and linewidth were determined in the nonirradiated materials using a tungsten-metal target with tungsten-compound absorbers. These parameters were compared to those obtained by observing the Mössbauer effect using tungsten-compound targets and tungsten-metal absorbers. Anomalous hyperfine interactions were observed in all irradiated compounds. The recoilless fraction was found to be reduced in most of the materials. In WO_3 it was found that the fractional reduction in recoilless fraction does not depend on the γ-ray energy and is time independent. The data can be understood in terms of the formation of locally amorphous regions associated with the Coulomb-excited nuclei.

I. INTRODUCTION

The problem of determining the interaction of energetic particle radiation with solids has received considerable attention over the past several years. The theoretical description of the problem usually has begun with an analysis of the initial collision cascade. Ion ranges and damage distributions have been evaluated[1] for various collision cross sections and projectile-to-target mass ratios. Computer simulations of the collision cascade have been generated[2,3] with various initial conditions and interatomic potentials for several types of lattices. These calculations find "spike" phenomena. The displacement spike, originally proposed by Brinkman,[4] involves the removal of many ions from their original lattice sites. The less dramatic thermal spike, proposed by Seitz,[5] involves fewer displacements with the creation of Frenkel pairs. Large local temperature increases of short duration are associated with these spikes. At present there is no general agreement on the details and magnitude of the collision cascade, local temperature increase, and subsequent annealing for most materials.

Although the models often deal with short-time microscopic behavior of solids, most experiments do not. Experimental investigation has been largely macroscopic, with measurements being made a long time after irradiation. Much work has been done to study the subsequent annealing in these experiments.[6] For example, release-of-inert-marker-gas studies[7] have yielded information about the final state of the material. Changes in electrical resistivity[8] and bulk changes in the material have been observed following irradiation.

To study the short-time effect of radiation damage, it is necessary to make use of the short lifetimes of nuclear states. The techniques of perturbed angular correlation[9] and the Mössbauer effect provide methods of microscopically investigating the material following irradiation. The Mössbauer effect[10] is sensitive to the hyperfine field of the emitting nucleus and the chemical environment, and also reflects the mean-square atomic displacement through the recoilless fraction f. In this way the Mössbauer effect serves as a microscopic probe of the environment of the emitting nucleus. We can make a distinction between two types of Mössbauer-effect measurements. Radiation damage may occur either during the production of a parent nucleus or during the excitation of the Mössbauer level. When a parent nucleus is involved (e.g., reactor produced), the Mössbauer level decays a long time after irradiation. When the Mössbauer level is excited directly (e.g., α decay from annealed sources or Coulomb excitation), the Mössbauer level decays immediately.

An early experiment by Stone and Pillinger[11] attributed a reduced f observed following α decay, as compared with the f observed following β decay in NpO_2, to radiation damage associated with α-particle emission. However, Mullen[12] suggested that the reduction in f was caused by an increase in temperature caused by the α decay rather than ion displacement.

An alternative to radioactive Mössbauer sources is provided by Coulomb excitation. The advantages of resonant absorption (and emission) following Coulomb excitation (RACE) over macroscopic radiation-damage probes and radioactive-source experiments are the following: (i) RACE experiments provide information at a time on the order of the lifetime of the nuclear state. It is possible, owing to this short time scale, to investigate spike phenomena. (ii) Since the Mössbauer effect is sensitive to nuclear hyperfine interactions and atomic mean-square displacements, it is possible to determine whether the Mössbauer nuclei have decayed from sites in defected environments. (iii) The observed damage is produced by the lattice

ion recoiling after Coulomb excitation. The pro-
jectile ion stops far from this region of damage
so no impurities are introduced in the vicinity of
the Mössbauer decay.

Several investigators[13-15] have reported broadened
Mössbauer spectra following Coulomb excitation,
and have attributed this broadening to the Möss-
bauer nuclei decaying from sites which are dam-
aged. Jacobs and Hershkowitz[16] observed anoma-
lous hyperfine interaction in various hafnium com-
pounds. The most striking examples were HfC
and HfN, which both showed substantial broadening.
Günther et al., using perturbed-angular-correla-
tion techniques, also observed anomalous hyper-
fine interactions in irradiated hafnium metal.[17]
They attributed the observed reduction in the hy-
perfine interaction to γ decay from a distribution
of sites. Recently Hardy et al.[18] attributed the
lack of resonant absorption in Ho_2O_3 ($\tau_{1/2} \approx 20$ psec),
and the reduction of f in Lu_2O_3 and Er_2O_3 ($\tau_{1/2}$
≈ 100 psec) following Coulomb excitation, to tem-
perature increases associated with the collision
cascade.

We have found similar reductions in f's in tung-
sten compounds. In the case of WO_3, we have
previously reported[19] that the fractional reduction
in f remains essentially constant between 0.15 and
1.3 nsec following the Coulomb excitation. This
reduction in f can be understood in terms of the
formation of amorphous regions surrounding the
decaying nucleus. This assumption was shown to
be consistent with the results of macroscopic
experiments.

In this paper we report the results of RACE ex-
periments on WC, WB, W_2B, W_2B_5, WS_2, and
WO_3. The lifetimes and transition energies of
the tungsten isotopes studied are 1.37 nsec, 100.1
keV for W^{182}; 1.28 nsec, 111.2 keV for W^{184}; 1.01
nsec, 122.6 keV for W^{186}; and 0.15 nsec, 46.48
keV for W^{183}. The even-even isotopes, because of
their relatively long lifetimes, have absorption lines
narrow enough to resolve and yield some informa-
tion about hyperfine fields. Since the lifetime of
the W^{183} isotope is short, the hyperfine field is not
observable, but short-time behavior of the re-
coilless fractions is. We have determined the
long-time (approximately 1.3 nsec) and the short-
time (0.15 nsec) behavior of the recoilless frac-
tions of irradiated and nonirradiated WC and WO_3.
The hyperfine interactions in WC, WO_3, WB, W_2B,
W_2B_5, WO_3, and WS_2 were measured at the even-
even isotope time scale for both the irradiated and
nonirradiated conditions.

II. EXPERIMENTAL CONFIGURATION

The experimental apparatus is essentially the
same as described previously.[16] Targets and ab-
sorbers were cooled to approximately 20 °K (mea-

sured by a copper-constantan thermocouple) with
a closed-cycle helium refrigerator.[20] The first
excited states of W^{182}, W^{184}, W^{186} and W^{183} were
Coulomb excited with a 6.0-MeV singly charged
He^4 beam produced by the University of Iowa CN
Van de Graaf accelerator. Beam currents were
approximately 1 μA for tungsten-metal targets and
approximately 400 nA for tungsten-compound tar-
gets. The duration of each experiment was several
days.

The Mössbauer spectrometer was driven in the
constant-acceleration mode. Since the natural
abundance, lifetimes, and energies of the first ex-
cited states of even-even tungsten isotopes studied
are similar, data for each transition were acquired
simultaneously into a quarter of a multiscaling
analyzer. An Fe^{57} velocity calibration was also
simultaneously acquired into the fourth quarter
of the analyzer.

Targets for the experiments were made by mix-
ing the tungsten compound in powder form with
epoxy[21] and gluing it to a copper target blank. The
tungsten-metal target consisted of a 0.01-cm-thick
natural-tungsten-metal foil glued to a target blank.
The absorbers used were made by mixing the tung-
sten compound with epoxy and gluing into an ab-
sorber blank. The tungsten-metal absorber con-
sisted of a 0.008-cm-thick piece of natural-tung-
sten metal. The following tungsten-compound ab-
sorbers with indicated crystal structures and
thicknesses were used in this set of experiments:
WC, hcp, 136 mg/cm^2; WB, tetragonal, 148 mg/
cm^2; W_2B, tetragonal, 144 mg/cm^2; W_2B_5, hcp,
161 mg/cm^2; WO_3, monoclinic, 93 mg/cm^2; WS_2,
hexagonal, 265 mg/cm^2. The crystal structures
of the compounds[22] were confirmed from Debye-
Scherrer x-ray powder diffraction patterns.

III. RESULTS

A. General

Measurements of radiation-damage effects in
the various tungsten compounds were performed
in the following manner. RACE spectra using a
tungsten-metal target with tungsten-compound ab-
sorbers were obtained. Results of these target-
absorber combinations gave the nonirradiated
parameters of the tungsten compounds. These
parameters were then compared to those obtained
using tungsten-compound targets with a tungsten-
metal absorber. Differences between the irradi-
ated and nonirradiated parameters were attributed
to radiation-damage effects.

Tungsten metal, which is cubic in structure, has
been shown[23] to produce narrow single-line RACE
spectra with tungsten-metal absorbers. The
Mössbauer spectra do not show evidence of radia-
tion damage. Either such disorder has healed
within the lifetime of the transition or the technique

is not sensitive to such damage. Since the *target* has a narrow single line, the spectra observed using a tungsten-metal target with a tungsten-compound absorber reflect the hyperfine interaction in the absorber and the data were least-squares fit to sums of single Lorentzians constrained for electric quadrupole interaction in the absorber. In no case was the hyperfine field great enough to resolve the absorption lines. We have previously[24] shown that under these conditions the approximation of fitting the data to sums of Lorentzians is not valid. The fits were corrected using a graphical technique[25] developed to describe partially resolved hyperfine interactions in the absorber. This procedure yields the correct hyperfine interaction $\frac{1}{4}eQV_{zz}$ and effective thickness t of the absorber if the source width and source f are known. It does not accurately determine the asymmetry parameter η. Values for the width and f of the tungsten-metal target were determined from experiments using a tungsten-metal target with a tungsten-metal absorber.

The recoilless fraction of the nonirradiated material (i.e., when used as absorbers) f_{nt} can be found since $t = n\sigma f_{nt}$, where n is the number density and σ is the cross section.

The widths Γ_{irr}, hyperfine interaction $(\frac{1}{4}eQV_{zz})_{irr}$, and recoilless fraction f_{irr} observed following irradiation were obtained from RACE spectra using tungsten-compound targets with a tungsten-metal absorber. In these experiments the Mössbauer spectra were least-squares fit to sums of single-line Lorentzians constrained for electric quadrupole interaction in the target. The irradiated hyperfine interaction is directly obtainable from these fits. The area α under the spectrum when corrected for background gives the recoilless fraction of the source since $\alpha = f_{irr}A(t)$.[26] $A(t)$ only depends on the 0.008-cm-thick tungsten-metal absorber and was determined from experiments using a tungsten-metal target with that tungsten-metal absorber.

The linewidth of the irradiated material can be found using the relationship[27]

$$\Gamma_{obs} = \Gamma_s + \Gamma_n(1 + 0.29t - 0.005t^2), \quad 4 < t < 10$$
$$\Gamma_{obs} = \Gamma_s + \Gamma_n(1 + 0.27t), \quad\quad\quad t < 4.$$ (1)

Γ_{obs} is the observed linewidth, Γ_s is the width of

the source (Γ_{irr}), Γ_n is the natural linewidth, and t is the effective thickness of the absorber. Γ_n has been determined[23] for W^{182}, W^{184}, and W^{186}. The effective thickness t was determined from experiments using a tungsten-metal target with a tungsten-metal absorber.

It we use the Debye model to describe the recoilless fraction data, the f for each isotope may be combined to give a single Debye temperature which characterizes the solid. Since the relative quadrupole moments of the even-even isotopes are known,[28] the electric field gradient V_{zz} may be expressed in terms of the quadrupole moment of W^{182}.

B. Results for Tungsten-Metal Target with Tungsten-Metal Absorber

Previous experiments[23] have determined the natural linewidths $2\Gamma_n$ for tungsten-metal absorbers to be 0.997 ± 0.01, 0.96 ± 0.01, 0.805 ± 0.07 mm/sec for W^{182}, W^{184}, and W^{186}, respectively. Since it has been shown[26] that the area of a Mössbauer spectrum is independent of the source width, we are free to let the source width equal the absorber width and write the area as[29]

$$\alpha = f_s[1 - e^{-t/2}J_0(it/2)] \, 2\Gamma_n(g(t)) \, ,$$
$$g(t) = 1 + 0.145t - 0.0025t^2, \quad 4 \le t \le 10$$
$$g(t) = 1 + 0.135t \, , \quad\quad\quad\quad t \le 4$$

and $t = n\sigma f_a$. If we assume the recoilless fraction of the source equals the recoilless fraction of the absorber, then the above expression can be solved numerically for t and f. Knowledge of the f's at each energy implies a Debye temperature Θ_D for tungsten metal at 20 °K equal to 319 ± 3 °K. If we assume that tungsten metal has a natural width as an absorber, Eq. (1) can be used to determine the source width since t has already been found. Since the area and recoilless fractions are known, $A(t)$ can be determined.

Table I summarizes the results obtained from the tungsten-metal-target-with-tungsten-metal-absorber experiment. For the four tungsten isotopes we determined the source width Γ_s, the recoilless fraction f (we assumed $f_s = f_a$), the effective thickness t of the absorber, and $A(t)$.

TABLE I. Parameters derived from tungsten-metal-target–with–tungsten-metal-absorber experiment.

	W^{182}	W^{182}	W^{186}	W^{183}
Γ_s (mm/sec)	1.02 ± 0.04	1.0 ± 0.14	1.01 ± 0.08	9.6 ± 2.3
f	0.186 ± 0.002	0.13 ± 0.01	0.088 ± 0.005	0.77 ± 0.09
t	5.60 ± 0.07	5.4 ± 0.4	3.8 ± 0.2	12.1 ± 1.4
$A(t)$	4.03 ± 0.1	3.8 ± 0.3	2.6 ± 0.2	100 ± 22

C. Results for Tungsten Compounds

The nonirradiated widths Γ_{ni}, hyperfine interactions $(\frac{1}{4}eQV_{zz})_{ni}$, and recoilless fraction f_{ni}, for the even-even isotopes, were obtained simultaneously using a tungsten-metal target with the tungsten-compound absorber and are listed in Tables II–IV. The nonirradiated widths, except for WS_2, agree with the natural widths.[23] The broadened width observed for WS_2 is attributed to geometric broadening[30] since that experiment was performed with poor collimation.

The hyperfine interactions for the nonirradiated tungsten compounds are listed in Table III. The V_{zz} component of the electric-field-gradient (EFG) tensor represents the weighted average of the three even-even tungsten isotopes in units of (volts) × (quadrupole moment of W^{182}). The values of the relative quadrupole moments were determined using the results of Oberley et al.[28]

The recoilless fractions for the nonirradiated tungsten compounds are given in Table IV. Debye temperatures calculated according to Hardy et al.[31] are listed in Table IV. The recoilless fractions of W^{183} were determined by using the Debye temperatures obtained from the even-even tungsten isotopes. We have checked this procedure by direct measurement of f in the case of W^{183} metal and $^{183}WO_3$ and find good agreement.

The irradiated widths Γ_{irr}, hyperfine interaction $(\frac{1}{4}eQV_{zz})_{irr}$, and recoilless fractions f_{irr} were determined from experiments using tungsten-compound targets and the tungsten-metal absorber. Values for Γ_{irr}, $(\frac{1}{4}eQV_{zz})_{irr}$, and f_{irr} are listed in Tables V–VIII. No resonant absorption (> 0.6%) was observed for the even-even isotopes in irradiated WS_2. The Debye temperatures $\Theta_{D,irr}$ were calculated using only the even-even isotope data.

TABLE II. Widths Γ_{ni} (mm/sec) from experiments using tungsten-metal targets with various tungsten-compound absorbers.

	W^{182}	W^{184}	W^{186}
WC	$0.58 ^{+0.06}_{-0.07}$	$0.50 ^{+0.19}_{-0.24}$	$0.45 ^{+0.12}_{-0.25}$
WB	$0.65 ^{+0.36}_{-0.32}$	$0.46 ^{+0.31}_{-0.31}$	
W_2B	$0.53 ^{+0.29}_{-0.10}$	$0.56 ^{+0.20}_{-0.25}$	$0.52 ^{+0.21}_{-0.20}$
W_2B_5	$0.52 ^{+0.12}_{-0.16}$	$0.38 ^{+0.34}_{-0.19}$	$0.57 ^{+0.33}_{-0.37}$
WO_3	$0.64 ^{+0.10}_{-0.10}$	$0.48 ^{+0.18}_{-0.18}$	$0.23 ^{+0.24}_{-0.21}$
WS_2	$0.97 ^{+0.10}_{-0.05}$	$0.82 ^{+0.12}_{-0.15}$	$0.88 ^{+0.21}_{-0.19}$

TABLE III. Hyperfine interaction $(\frac{1}{4}eQV_{zz})_{ni}$ and average $(V_{zz})_{ni}$ from experiments using tungsten-metal targets with various tungston-compound absorbers.

	W^{182}	W^{184}	W^{186}	$V_{zz} (\times 10^{-6})^a$
WC	$-1.62 ^{+0.04}_{-0.04}$	$-1.43 ^{+0.04}_{-0.24}$	$-1.24 ^{+0.06}_{-0.28}$	2.2 ± 0.1
WB	$0.86 ^{+0.17}_{-0.14}$	$0.97 ^{+0.10}_{-0.25}$		1.3 ± 0.3
W_2B	$-1.89 ^{+0.04}_{-0.05}$	$-1.61 ^{+0.06}_{-0.21}$	$1.38 ^{+0.08}_{-0.13}$	2.5 ± 0.1
W_2B_5	$1.48 ^{+0.03}_{-0.14}$	$1.21 ^{+0.06}_{-0.34}$	$1.07 ^{+0.08}_{-0.08}$	2.0 ± 0.2
WO_3	$-2.07 ^{+0.04}_{-0.05}$	$-1.86 ^{+0.05}_{-0.06}$	$-1.74 ^{+0.12}_{-0.13}$	2.8 ± 0.1
WS_2	$2.43 ^{+0.01}_{-0.02}$	$2.11 ^{+0.01}_{-0.02}$	$1.79 ^{+0.02}_{-0.03}$	3.2 ± 0.3

[a]In units of (volts) × (quadrupole moment of W^{182}).

There is no evidence of any nuclear reaction occurring for WC, WO_3, and WS_2 targets. However, irradiation of the tungsten boride compounds results in a 170-keV line indicating a $B^{10}(\alpha, p)C^{13}$ reaction; a high neutron flux and a 511-keV line indicated a $B^{10}(\alpha, n)N^{13}$ reaction.

There is good agreement between the irradiated widths and the source width of tungsten metal except for WC, which is slightly broader. In all cases the EFG is greater in the irradiated compounds than in the nonirradiated compounds. A striking feature of the hyperfine fields is that, except for the relatively low melting WO_3, all the EFG's in the irradiated compounds are the same within statistical uncertainties. The recoilless fractions of the irradiated tungsten compounds, with the exception of WB, are all significantly less than the EFG's in the nonirradiated materials.

IV. DISCUSSION

The bombardment of a tungsten compound with 6.0-MeV α particles creates a flux of tungsten recoil nuclei within the material. The average recoil energy of a Coulomb-excited tungsten atom is approxmately 200 keV. The maximum recoil energy is 480 keV, corresponding to 180° scattering. By folding the energy dependence of the Coulomb-excitation cross section with the energy loss of the incident α particle, it can be shown that more than half the Coulomb excitation occurs within the first 8 mg/cm² of target material.[16] Since the range of a 6.0-MeV α particle in tungsten is approximately 21 mg/cm², we conclude that the α particles stop far from the region of Coulomb excitation.

We calculate the Coulomb-excited tungsten-atom recoil flux to be approximately 2×10^{13} (recoils/h)/μA. Most of the elastic recoils have energies less than the Coulomb-excited nuclei.

Using the results of calculations by Winterbon

TABLE IV. Recoilless fraction f_{ni} and corresponding Debye temperature $\Theta_{D,ni}$ from experiments using tungsten-metal targets with various tungsten-compound absorbers.

	W^{182}	W^{184}	W^{186}	$\Theta_{D,ni}$ (°K)	W^{183}
WC	$0.22 \, {}^{+0.03}_{-0.02}$	$0.16 \, {}^{+0.10}_{-0.07}$	$0.13 \, {}^{+0.11}_{-0.05}$	$354 \, {}^{+47}_{-35}$	0.72 ± 0.03
WB	$0.10 \, {}^{+0.07}_{-0.04}$	$0.06 \, {}^{+0.07}_{-0.03}$		$239 \, {}^{+78}_{-45}$	
W_2B	$0.20 \, {}^{+0.01}_{-0.02}$	$0.14 \, {}^{+0.07}_{-0.05}$	$0.10 \, {}^{+0.05}_{-0.06}$	$333 \, {}^{+18}_{-33}$	
W_2B_5	$0.25 \, {}^{+0.12}_{-0.06}$	$0.20 \, {}^{+0.18}_{-0.12}$	$0.13 \, {}^{+0.27}_{-0.10}$	$388 \, {}^{+218}_{-95}$	
WO_3	$0.075 \, {}^{+0.01}_{-0.01}$	$0.039 \, {}^{+0.014}_{-0.017}$	$0.016 \, {}^{+0.016}_{-0.016}$	$215 \, {}^{+16}_{-9}$	0.57 ± 0.007
WS_2	$0.06 \, {}^{+0.007}_{-0.007}$	$0.04 \, {}^{+0.01}_{-0.01}$	$0.03 \, {}^{+0.02}_{-0.01}$	$207 \, {}^{+13}_{-12}$	0.61 ± 0.02

et al.,[1] we estimate the spatial extent of the damage caused by a 200-keV tungsten atom in tungsten to be approximately 1.3×10^{-20} cm^3. Since the majority of the data come from the first 8 mg/cm^2 of the target, the total effective volume of the target is 10^{-3} cm^3. If we assume that the damage is uniformly created in the first 8 mg/cm^2, then the ratio of damaged volume to effective volume, including elastic recoils, is less than 1%, since the irradiation never exceeded 50 μA h. As a result of this the recoiling Mössbauer nuclei decay in regions of damage *they* created and do not interact with other damaged regions.

A. Recoilless Fractions

The recoilless fraction f can be expressed as $f = e^{-k^2 \langle x^2 \rangle}$, where $k = E_\gamma / \hbar c$ and $\langle x^2 \rangle$ is the mean-square atomic displacement. Using the Debye model, $\langle x^2 \rangle$ can be expressed in terms of the Debye temperature, the mass of the atom, and the ambient temperature of the solid. An empirical relationship between f and the parameters of the Debye model is given by Hardy *et al.*[31] If different γ-ray energies are investigated for the same isotope in the same material, one would expect to find the same mean-square atomic displace-

ment. There are two possible reasons for the recoilless fractions of different γ-ray transitions not to correspond to a unique mean-square displacement or Debye temperature. First, the mean-square displacement may be time dependent. Second, the nuclei may decay from different sites with different mean-square atomic displacements.

Figure 1 shows a plot of the recoilless fractions observed for the W^{182} transition in the irradiated and nonirradiated tungsten compounds. W^{184} and W^{186} follow the same trend but have larger errors. Reductions in f for the even-even isotopes were observed following irradiation in WC, W_2B, W_2B_5, WO_3, and WS_2. No reductions were observed in irradiated WB. Reductions in f were also observed for the short-lived W^{183} in WO_3 and WC.

We have previously reported[19] unsuccessful attempts to attribute the reduction in f to local-temperature increase in the case of WO_3. In addition, the reduction in f following irradiation cannot be attributed to a unique increase in the mean-square atomic displacement. We found no single mean-square displacement which would predict the observed f's for W^{183} and W^{182} in irradiated WO_3.

We measured the fractional reduction in f, $f_{irr}/$

TABLE V. Width Γ_{irr} (mm/sec) from experiments using various tungsten-compound targets with tungsten-metal absorbers.

	W^{182}	W^{184}	W^{186}
WC	1.29 ± 0.16	1.08 ± 0.22	1.38 ± 0.39
WB	1.17 ± 0.25	1.35 ± 0.42	1.07 ± 0.41
W_2B	0.86 ± 0.25	1.01 ± 0.42	3.92 ± 1.5
W_2B_5	1.51 ± 0.66	1.65 ± 1.01	0 ± 0.31
WO_3	1.63 ± 0.7[a]		

[a]Enriched isotope.

TABLE VI. Magnitude of the observed hyperfine interactions $(\frac{1}{4}eQV_{zz})_{irr}$ (mm/sec) from experiments using various tungsten-compound targets with tungsten-metal absorbers.

	W^{182}	W^{184}	W^{186}
WC	2.59 ± 0.11	2.11 ± 0.13	1.36 ± 0.47
WB	2.26 ± 0.15	2.27 ± 0.2	1.87 ± 0.2
W_2B	2.31 ± 0.13	1.87 ± 0.3	3.3 ± 0.46
W_2B_5	2.57 ± 0.54	2.0 ± 0.6	1.6 ± 0.2
WO_3	3.41 ± 0.43		

TABLE VII. Recoilless fractions f_{irr} and corresponding Debye temperature $\Theta_{D,irr}$ from experiments using various tungsten-compound targets with tungsten-metal absorbers.

	W^{182}	W^{184}	W^{186}	$\Theta_{D,irr}$ (°K)	W^{183}
WC	0.132 ± 0.013	0.08 ± 0.01	0.056 ± 0.009	268^{+14}_{-14}	0.55 ± 0.14
WB	0.187 ± 0.02	0.10 ± 0.02	0.062 ± 0.13	293^{+17}_{-17}	
W_2B	0.094 ± 0.01	0.049 ± 0.009	0.069 ± 0.03	231^{+11}_{-11}	
W_2B_5	0.22 ± 0.04	0.079 ± 0.025	0.025 ± 0.008	246^{+17}_{-21}	
WO_3	0.025 ± 0.004^a			$162^{+6}_{-6}{}^b$	0.29 ± 0.08
WS_2					0.31 ± 0.1

[a]Enriched isotope.

[b]Represents average of low-velocity-enriched-target and high-velocity-natural-target experiments.

f_{ni}, for W^{182} to be 0.33 ± 0.06, and f_{irr}/f_{ni} for W^{183} to be 0.51 ± 0.15, in WO_3. The equality of the two ratios suggests that the recoiling nuclei decay from two types of sites in the irradiated material. One kind of site has a recoilless fraction which is comparable to the nonirradiated value; the other site has a much smaller f.

Results of experiments on WC are more ambiguous. The short-time (0.15 nsec) W^{183} fractional reduction was measured to be 0.76 ± 0.2. The long-time (1.3 nsec) W^{182} fractional reduction is 0.6 ± 0.1. While these fractional reductions are equal within statistical uncertainty, a unique mean-square displacement corresponding to a Debye temperature of 268 ± 15 °K also can account for the f's observed for W^{182}, W^{184}, W^{186}, and W^{183} in WC. It is therefore not possible to determine whether the reduction in f is due to an overall increase in the atomic mean-square displacement or γ emission from different sites.

Unfortunately, the short-lived W^{183} transition cannot be investigated in the tungsten boride compounds owing the large background resulting from nuclear reactions.

B. Widths

Figure 2 shows a plot of the widths of the W^{182} transition for both irradiated (targets) and non-irradiated (absorbers) tungsten compounds. Except for WS_2, the widths of all the nonirradiated compounds are the same, and agree with the natural width of the state as determined by Mekshes and Hershkowitz.[23] The broader value obtained in the WS_2 experiment can be attributed to geometric broadening[30] since that experiment was the only one performed with poor collimation.

The widths of the lines in the irradiated materials, with the exception of WC, are all the same within the uncertainty of their measurement, and agree with the width of irradiated tungsten metal. The irradiated widths (source widths) are approxi-

TABLE VIII. The lower limit M of the fraction of nuclei which decay in EFG's not present in nonirradiated material from experiments using various tungsten-compound targets with tungsten-metal absorbers.

	W^{182}	W^{184}	W^{186}	Average M
WC	0.3 ± 0.1	0.2 ± 0.1	0.2 ± 0.1	0.23 ± 0.06
WB	0.38 ± 0.07	0.38 ± 0.1		0.38 ± 0.06
W_2B	0.02 ± 0.12	0.13 ± 0.26	0.46 ± 0.25	0.1 ± 0.1
W_2B_5	0.32 ± 0.13	0.27 ± 0.24		0.3 ± 0.1
WO_3	0.37 ± 0.15^a			0.37 ± 0.15

[a]Enriched isotope.

FIG. 1. Recoilless fraction of W^{182} for tungsten compounds.
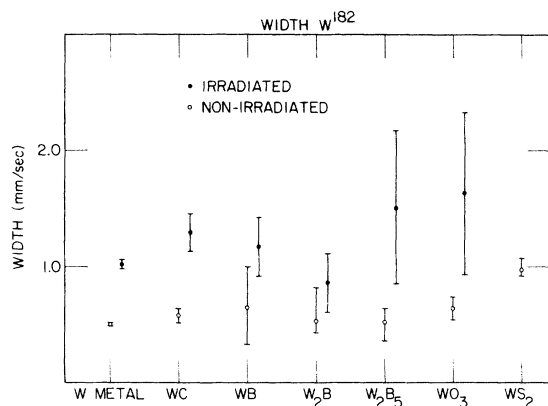
FIG. 2. Widths of W^{182} transitions for tungsten compounds.

mately twice the natural linewidth. The broadening of the source width can be attributed to a combination of velocity smearing[32] and self-absorption in the source.

The broadened width in the case of WC can be attributed to resonant emission from several different sites with different EFG's. Since the data were fit with one unique hyperfine interaction, any deviation from that assumption would be reflected in a broadened width. This suggests that in WC resonant emission occurs from more than one site subject to different EFG's. In the other compounds which have the same source width within statistical uncertainty as tungsten metal, resonant emission is then consistent with decay from sites which have essentially the same EFG's. Thus the width of the line is an indication of the range of EFG's associated with resonant emission.

C. Hyperfine Interactions

The EFG's determined from the irradiated and nonirradiated tungsten compounds are plotted in Fig. 3. Perhaps the most striking observation is that the EFG's in irradiated WC, WB, W_2B, and W_2B_5 are the same within uncertainties, even though the EFG's in the nonirradiated materials are different. In all cases the EFG's in the irradiated materials were greater than those in the nonirradiated materials. The differences range from a 25% increase in W_2B to a 140% increase in WB.

It is possible, however, to estimate the fraction of nuclei, M, which decay subject to EFG's that are *not* present in the nonirradiated material. We can construct a spectrum corresponding to a tungsten-compound source and a tungsten-metal absorber, with the same hyperfine interaction as the nonirradiated material, a width equal to the tungsten-metal width but whose source recoilless fraction is the same as that observed in the damaged

configuration. This spectrum can be scaled to have the same depth at zero velocity as the observed damaged spectrum. The ratio M of the difference in areas of the two spectra to the area of the damaged spectra represents a lower limit on the fraction of nuclei which decay in EFG that are not present in the nonirradiated material. As an example of this analysis, consider $W^{182}C$. The hyperfine interaction for nonirradiated WC is 1.62 ± 0.04 mm/sec. The fraction M can be written as $1 - 5\pi h'w'(d/d')/5\pi hw$. The depths h, h' and the widths w, w' refer to the observed radiation-damaged spectrum and the constructed spectrum, respectively. d and d' are the depths at zero velocity of the observed and constructed spectra, respectively. The width w' is the width one would observe if WC were used as a target, and not damaged, using the 0.008-cm-thick tungsten-metal absorber. This width has been determined from the tungsten-metal-target-with-tungsten-metal-absorber experiment to be 2.25 ± 0.4 mm/sec. Since the only difference between the constructed spectrum and the observed spectrum is the hyperfine interaction, the area of the two spectra are equal. h' is then equal to $hw/w' = 0.015 \pm 0.001$. Knowing h, w', and the hyperfine interaction in $W^{182}C$, the depth at zero velocity, d', may be found:

$$d' = \sum_{i=1}^{5} \frac{h'w'^2}{x_i^2 + w'^2} = 0.053 \pm 0.005 \, ,$$

where x_i are the positions of the five absorption lines. The depth at zero velocity in the irradiated situation, d, is measured to be 0.038 ± 0.003. The fraction M is given by $1 - d/d' = 0.3 \pm 0.1$.

Values of M for each isotope and compound are listed in Table VIII. W_2B has the smallest fraction of nuclei which might decay at sites different from the nonirradiated material, $M = 0.1 \pm 0.1$, while WB shows the largest fraction, $M = 0.38 \pm 0.06$.
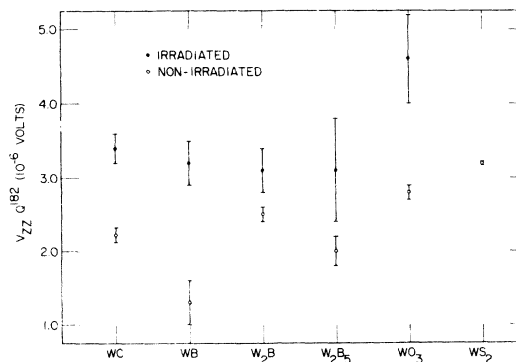
FIG. 3. $V_{zz}Q^{182}$ for tungsten compounds.

D. Locally Amorphous Regions

One possible explanation for the results of these experiments is the formation of locally amorphous regions. Such an explanation is suggested by the results of macroscopic measurements made by Kelly and Lam[33] on WO_3. They have shown that WO_3 becomes locally amorphous when between 9 and 17% of the atoms are locally displaced from their lattice sites during the initial collision cascade. Amorphous regions are characterized by a lack of crystal structure. Resonant emission is, however, still possible if $\langle x^2 \rangle$ is small enough. With greater atomic diffusion in such amorphous regions, the recoilless fraction would be reduced. In fact, substantial increases in diffusion in such regions are sometimes possible. Ruby, Zabransky, and Stevens[34] report that experiments on frozen aqueous solutions show a change with temperature from an amorphous phase, in which resonant absorption is observed, to a supercooled liquid phase where diffusion is so great that the Mössbauer effect is not observed.

The Mössbauer parameters expected from recoilless emission in such amorphous regions are the following: (i) possible, but not necessary, reductions in f, (ii) a range of hyperfine fields because of the lack of crystal structure, and (iii) a broadened width owing to a range of hyperfine fields (since isomer shifts found in tungsten compounds are too small to account for broadening). Broadened absorption widths have been reported in Mössbauer-effect studies on glasses.[35]

The Mössbauer parameters expected from a recrystallized region should be the same as in the nonirradiated material, except for possible temperature effects. However, calculations for WO_3 show that at the time of the decay, the ambient temperature has decreased to a value where the effect of the temperature increase is negligible.[19] Therefore such a description is not consistent with the increased hyperfine fields we observe.

If the Mössbauer nucleus decays in an amorphous region, it would be subject to a range of EFG's. These EFG's could be almost independent of the initial crystal structure, as is found in these experiments. For the case of the three tungsten borides, we would expect that the same EFG's exist in the amorphous state even though the undamaged EFG's are quite different, as is seen in the experiment.

Jacobs and Hershkowitz[16] found the same consistency in hyperfine fields in hafnium compounds. The hyperfine interactions for irradiated HfB_2, HfC, and HfO_2 were within 10% of each other, although their nonirradiated fields were very different. In addition, the hyperfine fields observed following irradiation in those Hf compounds are

similar in magnitude to the fields observed in irradiated tungsten compounds.

E. Sensitivity of This Technique

We have already noted that no evidence of recoil radiation damage was found in tungsten metal. However, several investigators, using internal-friction methods,[36,37] have shown that the irradiation of tungsten metal can produce noticeable effects. These are present a long time after irradiation.

The RACE technique is sensitive to a different aspect of irradiation damage. It looks *only* at the environment of excited nuclei responsible for the collision cascades, and only at nuclei which are relatively tightly bound. In addition, the time scale is the nuclear lifetime, here about 1 nsec. It is not sensitive to irradiation damage if it is only present in the neighborhood of a few percent of these nuclei, because of statistical uncertainties in the data. It is basically a measurement of the environment of the average tightly bound nuclei but it also tells what fraction are tightly bound. It is therefore not surprising that other techniques which are sensitive to defects find evidence of irradiation damage in tungsten metal that we do not. The observation of damage in tungsten compounds reported in this paper indicates that a *large* fraction of the nuclei are in damaged environments 1 nsec after the collision cascade. In tungsten metal *most* tungsten nuclei do not appear to be in damaged environments on this time scale.

V. CONCLUSIONS

RACE spectra were observed for the even-even tungsten isotopes using a tungsten-metal target with W metal, WC, WB, W_2B_5, WO_3, and WS_2 absorbers. Since tungsten metal shows no evidence of radiation damage during irradiation, the recoilless fraction, Debye temperatures, and EFG's of those compounds were determined in nonirradiated environments.

To determine the effect of irradiation on these compounds, RACE spectra from the even-even tungsten isotopes were investigated using WC, WB, W_2B, W_2B_5, WO_3, and WS_2 as targets with a tungsten-metal absorber. No resonant absorption was observed for WS_2. Increases in hyperfine interactions were observed in all cases. The recoilless fractions were found to be smaller than their nonirradiated values in WC, W_2B, W_2B_5, and WO_3. Results of experiments on the short-lifetime state in W^{183} indicate that the reduction in recoilless fraction is the same between 0.15 and 1.4 nsec, and cannot be attributed to an increase in ambient temperature.

The observed reductions in f's and increases

in hyperfine fields both indicate that 1.3 nsec after the initial collision cascade the region surrounding the nucleus responsible for the damage has not recrystallized. The similarity of the anomalous hyperfine fields observed in all the compounds following irradiation indicates that the final states are the same and do not depend on the initial (non-irradiated) crystal structures of the materials.

These results are consistent with a model which predicts the presence of a locally amorphous region lasting at least 1.3 nsec after the collision cascade.

*Work supported in part by the National Science Foundation and the Research Corp.

†Present address: Tandam Accelerator Laboratory, McMaster University, Hamilton, Ontario, Canada.

[1] K. B. Winterbon, Peter Sigmund, and J. B. Sanders, K. Dan. Vidensk. Selsk. Mat.-Fys. Medd. 37, No. 14 (1970).

[2] C. Erginsoy, G. H. Vineyard, and A. Shimizu, Phys. Rev. 139, A118 (1965).

[3] J. R. Beeler, Jr., Phys. Rev. 150, 470 (1966).

[4] J. A. Brinkman, J. Appl. Phys. 25, 961 (1954).

[5] F. Seitz and J. S. Koehler, in Solid State Physics edited by H. Ehrenreich, F. Seitz, and D. Turnbull (Academic, New York, 1956), Vol. 2, p. 351.

[6] R. Kelly and H. M. Naguib, in Atomic Collision Phenomena in Solids, edited by D. W. Palmer, M. W. Thompson, P. D. Townsend (North-Holland, Amsterdam, 1970), p. 172.

[7] E. V. Kornelson, Can. J. Phys. 48, 2812 (1970).

[8] J. Ponsoye, Radiat. Eff. 8, 13 (1971).

[9] B. Herskind, in Hyperfine Interactions in Excited Nuclei, edited by G. Goldring and R. Kalish (Gordon and Breach, New York, 1971), p. 987.

[10] G. K. Wertheim, A. Hausman, and W. Sander, Electronic Structure of Point Defects in Crystalline Solids (North-Holland, Amsterdam, 1971), Series Vol. 4.

[11] J. A. Stone and W. L. Pillinger, Phys. Rev. Lett. 13, 200 (1964)

[12] J. G. Mullen, Phys. Lett. 15, 15 (1965).

[13] W. H. Wiedemann, P. Kienle, and F. Stanek, Z. Angew. Phys. 15, 7 (1963).

[14] P. Hannaford, C. J. Howard, and J. W. G. Wignall, Phys. Lett. 19, 257 (1965).

[15] E. T. Ritter, P. W. Keaton, Jr., Y. K. Lee, R. R. Stevens, Jr., and J. C. Walker, Phys. Rev. 154, 287 (1967).

[16] C. G. Jacobs, Jr. and N. Hershkowitz, Phys. Rev. B 1, 839 (1970).

[17] C. Günther, B. Skaali, R. Bauer, and B. Herskind, Nucl. Phys.

A. 164, 321 (1971).

[18] K. A. Hardy, J. C. Walker, and R. Schnidman, Phys. Rev. Lett. 29, 622 (1972).

[19] S. A. Wender and N. Hershkowitz, Phys. Rev. Lett. 29, 1648 (1972).

[20] Cryodyne 1020, manufactured by Cryogenic Technology, Inc., Waltham, Mass.

[21] C-7 epoxy with Activator V, manufactured by Armstrong Products, Warsaw, Ind.

[22] Purchased from A. D. McKay, Inc., New York, N. Y.

[23] M. Mekshes and N. Hershkowitz, Phys. Rev. C 2, 289 (1970).

[24] S. A. Wender and N. Hershkowitz, Nucl. Instrum. Methods 98, 105 (1972).

[25] N. Hershkowitz, R. D. Ruth, S. A. Wender, and A. B. Carpenter, Nucl. Instrum. Methods 102, 205 (1972).

[26] S. S. Hanna and R. S. Preston, Phys. Rev. 139, 722 (1965).

[27] D. A. O'Connor, Nucl. Instrum. Methods 21, 318 (1963).

[28] L. Oberley, N. Hershkowitz, S. A. Wender, and A. B. Carpenter, Phys. Rev. C 3, 1585 (1971).

[29] A. J. F. Boyle and H. E. Hall, Rep. Prog. Phys. 25, 469 (1962).

[30] N. Hershkowitz, Nucl. Instrum. Methods 53, 172 (1967).

[31] K. A. Hardy, F. T. Parker, and J. C. Walker, Johns Hopkins University Research Report, October, 1970 (unpublished).

[32] S. A. Wender and N. Hershkowitz, Nucl. Instrum. Methods 93, 571 (1971).

[33] R. Kelly and Nghi Q. Lam, Radiat. Eff. 10, 247 (1971).

[34] S. L. Ruby, B. J. Zabransky, and J. G. Stevens, J. Chem. Phys. 54, 4559 (1971).

[35] K. P. Mitrofanov and T. A. Sidonov, Fiz. Tverd. Tela 9, 890 (1967) [Sov. Phys.-Solid State 9, 693 (1967)].

[36] J. A. di Carlo and J. R. Townsend, Acta Metall. 14, 1715 (1966).

[37] J. A. di Carlo, C. L. Snead, and A. N. Goland, Phys. Rev. 178, 1059 (1969).